J|A|C|S COMMUNICATIONS

Published on Web 12/07/2010

# A Porous Metal−Organic Replica of α-$PbO_2$ for Capture of Nerve Agent Surrogate

Ruqiang Zou,*[,†,‡] Ruiqin Zhong,[‡] Songbai Han,[§] Hongwu Xu,[‡] Anthony K. Burrell,[‡] Neil Henson,[‡] Jonathan L. Cape,[‡] Donald D. Hickmott,[‡] Tatiana V. Timofeeva,[||] Toti E. Larson,*[,‡] and Yusheng Zhao*[,‡]

*Department of Advanced Materials and Nanotechnology, Department of Energy and Resources Engineering, College of Engineering, Peking University, Beijing 100871, China, Earth and Environmental Sciences Division, Los Alamos Neutron Science Center, Materials Physics and Applications Division, and Theoretical Division, Los Alamos National Laboratory, Los Alamos, New Mexico 87545, United States, Neutron Scattering Laboratory, China Institute of Atomic Energy, Beijing 102413, China, and Department of Chemistry, New Mexico Highlands University, Las Vegas, New Mexico 87701, United States*

Received February 18, 2010; E-mail: rzou@pku.edu.cn; tlarson@lanl.gov; yzhao@lanl.gov

***Abstract:*** A novel metal-organic replica of α-$PbO_2$ exhibits high capacity for capture of nerve agent surrogate.

Because of the availability of their precursors and their relative ease of synthesis, nerve agents comprise a class of toxic chemicals likely to be used by terrorist groups. The Sarin gas attack at the Tokyo subway station in May 1995 is a demonstration of the toxicity of nerve agents and their accessibility to terrorists. In addition to Sarin, there are a large number of other highly toxic organophosphate compounds that can be utilized as warfare or terror agents. Most of these compounds contain free phosphonic acid terminal groups or their phosphonate ester analogues. These molecules can form strong complexes with divalent metal ions (Ca, Mg, Zn, etc.), which is in part responsible for their toxicity in biological systems. Therefore, there has been an urgent need to develop new filtration technologies that reversibly capture and release a wide range of chemical threat agents, eliminating the need for traditional expendable media.

Our approach is to develop novel materials based on metal−organic frameworks (MOFs) to specifically recognize, bind, and capture nerve agents and their precursors. MOFs are a new family of crystalline porous materials, the structures of which are composed of metal-cluster units linked by organic ligands through strong coordination bonds.[1,2] The flexibility with which these components can be varied has led to an extensive class of MOF structures with ultrahigh specific surface areas, far exceeding those achieved by porous activated carbons, and other sorbent materials.[3−5] They also exhibit tunable pore size, a functionalized pore wall, and high thermal stability. Recent research shows that MOFs can be used for efficient sensing/detection and capture of a range of guest molecules, such as harmful gases and high explosives frequently at the ppm level.[6] The specific properties of these MOFs can be optimized by varying their cavity size and their polarity and by incorporating selective binding sites on frameworks. Selective binding can also be achieved by varying the coordination environments of the base metals or the nature of the base metals used in MOF syntheses. In particular, the base metals are commonly accompanied by organic solvent molecules at the coordination sites. These solvent molecules can be easily displaced to create high binding affinity sites that can be tailored to specifically targeted molecules (toxic or nontoxic). Furthermore, the binding capacity of a metal ion toward organophosphate increases with increasing the Lewis acidity of the metal ion.[7] It is, therefore, conceivable to design coordinately unsaturated MOFs based on divalent metal ions that can strongly bind organophosphate molecules containing both the ester and phosphonic acid groups. These materials will contain coordinately unsaturated metal sites that can bind target molecules. In this communication, we report a novel porous MOF with coordinately unsaturated zinc sites on the channel wall for highly efficient capture of one of the most important nerve agent surrogates, methylphosphonic acid (MPA), even at the ppm level. This result will open the door to use tailored MOFs for the capture of a wide range of nerve agents.

Treatment of DMF/$H_2O$ (DMF = *N*,*N*′-dimethylformamide) solution of zinc nitrate, calcium hydroxide, and benzene-1,3,5-tricaboxylic acid ($H_3BTC$) at 95 °C inside a Teflon-capped scintillation vial for 10 h yields large needle-like crystals with a composition of $[Zn_2Ca(BTC)_2(H_2O)_2](DMF)_2$ (**1**).[8] The purities of the bulk products are confirmed by elemental analysis (Found: C, 37.93%; N, 3.49%; Calcd: C, 37.70%; N, 3.67%) and powder X-ray diffraction (PXRD) measurements.[9] The PXRD patterns exhibit that there are some discrepancies of peak intensities and positions in low angles of **1** in comparison with the simulated patterns based on single crystal XRD data. Synchrotron XRD data of **1** were further collected at room temperature to investigate the phase purities.[9] The result indicates that the bulk sample of **1** is the same phase to the single crystal, in which there is a slight crystal structure derivation from Rietveld refinement. The derivation should be ascribed to the difference of test temperatures between a single crystal (183 K) and bulk powder of **1** (room temperature). Notedly, the host framework of **1** displays reasonable flexibility under various temperatures. Unfortunately, the solvent-free sample of **1** decomposed when exposed to the strong synchrotron beam, so its structure cannot be further refined. Furthermore, upon re-exposing the solvent-free **1** to DMF/$H_2O$, the PXRD pattern reverts to the as-made form, implying the open zinc sites are accessible to guest molecules.[9]

Structural analysis shows **1** crystallizes in the orthorhombic space group $C222_1$ and consists of 3-connected BTC ligands coordinating to trinuclear $Zn_2Ca$ clusters. The central Ca atom lies in a crystallographic 2-fold axis with a half occupation in an asymmetric unit. Each Ca atom is coordinated by six separate BTC ligands *via*

[†] Peking University.
[‡] Los Alamos National Laboratory.
[§] China Institute of Atomic Energy.
[||] New Mexico Highlands University.

 **10.1021/ja101440z** 

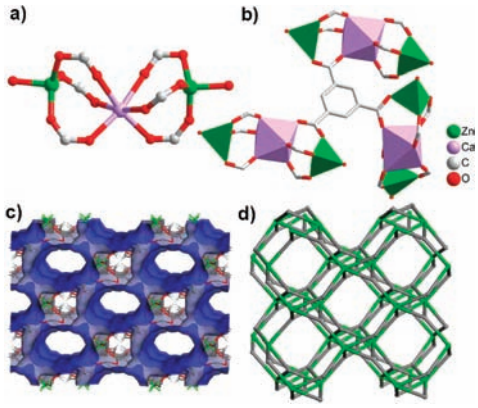


***Figure 1.*** Crystal structure of **1**: (a) trinuclear $Zn_2Ca(CO_2)_6(H_2O)_2$ cluster as a molecular building block (MBB), (b) coordination mode of the 3-connected BTC ligand, (c) three-dimensional molecular framework with open channels, and (d) unique α-$PbO_2$ topological net.

uniform monodentate carboxylate groups to form a pressed octahedron configuration (Figure 1a), and the terminal Zn atom adopts a tetrahedral coordination to link three separate BTC ligands and a water molecule. It should be noted that the $Zn-O_{water}$ bond (2.001(4) Å) is longer than those of $Zn-O_{carboxylate}$ bonds (an average value of 1.934 Å).[10] The $Ca-O_{carboxylate}$ bond lengths (2.319−2.433 Å) fall into the normal range.[10] The Zn···Ca separation (3.766(4) Å) in the trinuclear $Zn_2Ca(CO_2)_6$ cluster is longer than those of reported $Zn_3(CO_2)_6$ clusters (an average value of 3.366 Å).[10] The BTC ligand possesses a 3-connected geometry to link three $Zn_2Ca(CO_2)_6$ clusters in a uniform $\mu_2$ coordination mode of their carboxylate groups (Figure 1b). As a consequence, the metal clusters are interconnected by the ligands to generate a three-dimensional coordination framework with one-dimensional elliptical open channels, as illustrated in Figure 1c. The dimensions of the elliptical channel are 4.5 × 3.5 $Å^2$. Furthermore, DMF molecules are trapped in the open channels exhibiting a strong intermolecular H-bonding interaction with the coordinated water molecules (O1W−H1B...O6$^i$, $i = -x + 1.5, -y + 1.5, z + 0.5$). The total potential void volume of open channels in **1** is estimated to be about 45.2% based on the calculation of the potential solvent volume module using the *Platon* procedure.[11]

Interestingly, the linkage of the 6-connected $Zn_2Ca(CO_2)_6$ molecular building blocks (MBBs) and 3-connected BTC ligands in **1** leads to the formation of a unique metal−organic replica of the 3,6-connected α-$PbO_2$ topological net (Figure 1d). Based on our extensive search using the Cambridge Structural Database, the reported (3,6)-connected topological nets include rutile (rtl), Sit net, ryrite-like net (pyr), qom net, a $(4^3)(4.6^2)(4^4.6^8.8^3)$ net, a $(4.6^2)_2(4^2.6^9.8^4)$ net, a $(4.6^2)_2(4^2.6^{10}.8^3)$-c net, an anatase net (ant), and a H-bonding $(4.8^2)_2(4^2.8^{11}.10^2)$ net.[12] Thus, to the best of our knowledge, complex **1** represents the first case of metal−organic replica of 3,6-connected α-$PbO_2$ (apo) net.

Thermogravimetric analysis (TGA)[9] indicates that **1** loses its coordinate water molecules from 60 to 102 °C (Found: 5.20%; Calcd: 4.70%) and then no further weight loss happens up to 200 °C. The loss of the trapped DMF molecules occurs from 200 to 316 °C (Found, 18.94%; Calcd, 19.05%). The host framework starts to decompose rapidly from 430 °C. The high eliminating temperature of DMF indicates the strong interactions between DMF molecules and the host framework of **1**. PXRD patterns show that the original framework of the solvent-free **1** remains crystalline after activation at 300 °C for 12 h under vacuum.[9] When exposed to humid air, the solvent-free **1** sample immediately adsorbs water within several seconds. The new water can be easily removed by

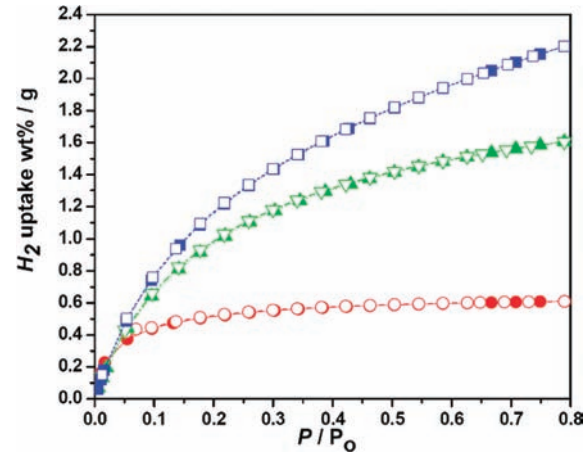


***Figure 2.*** Hydrogen adsorption isotherms of **1** at 77 K. **1a**−**c** represent the pretreated samples under various temperatures under vacuum for 12 h (**1a**, 120 °C (red); **1b**, 200 °C (green); and **1c**, 300 °C (blue)).

heating the sample to 120 °C under vacuum for 2 h. Compared with most of the MOFs where coordination sites are blocked by the structural ligands, **1** has the advantage that its coordinatedly unsaturated sites are on the interior of the channel walls. This results in two terminal Zn sites in each $Zn_2Ca$ cluster being accessible for guest adsorption.[7e]

The nitrogen adsorption isotherm of solvent-free **1** reveals a similar curve shape to those reported MOF compounds with the typical type-I adsorption behavior.[13] The Langmuir surface area,[14] BET surface area, and pore volume of **1** are 1075, 730 $m^2 \cdot g^{-1}$, and 0.47 $cm^3 \cdot g^{-1}$, respectively. The BET surface area (730 $m^2 \cdot g^{-1}$) is comparable to the simulated Connolly surface area (922 $m^2 \cdot g^{-1}$). Therefore, solvent-free **1** possesses the permanent porosity. Figure 2 shows the hydrogen adsorption isotherms of the pretreated **1** under various temperatures under vacuum. Samples **1a**, **1b**, and **1c** represent compound **1** with part or complete loss of the lattice solvent molecules. The result indicates that the encapsulated solvent molecules either occupy the open metal sites or block the pores of MOF to greatly reduce the hydrogen adsorption capacity of **1**. The solvent-free **1c** displays the excellent hydrogen uptake due to its coordinatedly unsaturated metal sites.

The adsorption isotherm of MPA was measured at various concentrations of MPA in dichloromethane/methanol (100:1) from 0 to 328 ppm using high performance liquid chromatography (Figure 3). Solvent-free **1** exhibits an excellent capacity for binding MPA. The MPA adsorption capacity of **1** first increases with increasing the mole ratio MPA/Zn and then reaches a plateau at a *ca.* 0.5−0.6 mol ratio of MPA/Zn, which is the saturated MPA adsorption in **1**. Notably, the title MOF extracts almost all MPA from the solution before the mole ratio MPA/Zn reaches 0.5. The detectable concentration of MPA in solution is 2−3 ppm after the adsorption of MPA in **1**. The saturated MPA adsorption density of 3.42 mmol/g in **1** is much higher than the reported results in goethite particles (0.084−0.2 mmol/g).[15]

We predict that the coordinatedly unsaturated Zn centers are the binding sites for MPA. Periodic density functional theory calculations were performed to investigate the exact adsorption sites/energies of MPA in **1** using the PBE0 function as implemented in the cp2k ab initio molecular simulation package.[16,17] Models for the simulation cell were constructed using a single unit cell of the experimentally determined crystal structure as a starting point with the coordinated water molecules removed to represent the calcined structure, which now has three-coordinate zinc centers. Two modes of binding of the MPA molecule were considered. The first binding

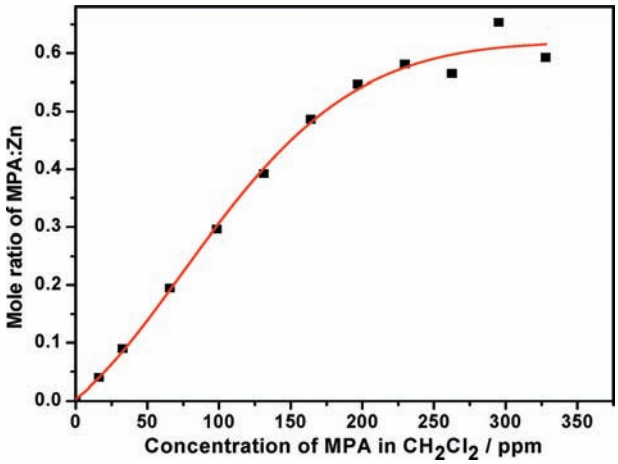


***Figure 3.*** Methylphosphonic acid adsorption in **1** at room temperature (red line represents the Gauss-fit curve).

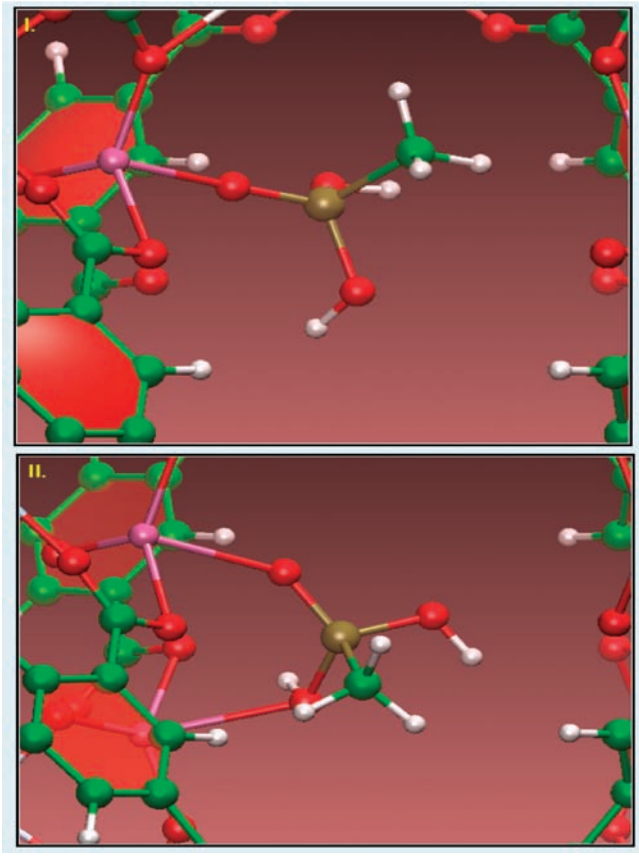


***Figure 4.*** Computed binding sites for MPA in **1**: (I) direct phosphoryl-Zinc coordination site and (II) bridging site (Zn, purple; O, red; H, white; C, green; P, tan).

site has the phosphoryl oxygen coordinated directly to the Zn site to produce a four-coordinate zinc center, and the second site also includes coordination of the hydroxyl oxygen to an adjacent zinc site from another $Zn_2Ca(CO_2)_6$ metal cluster. Cp2k uses a dual basis set of Gaussian-type orbitals and a plane-wave basis. Double zeta plus polarization basis sets were used for all atoms with Goedecker pseudopotentials with an energy cutoff of 280 Ry.[16] A basis set superposition correction was applied to the calculated binding energies using the counterpoise method. The calculated binding sites are shown in Figure 4. The two stable binding geometries are calculated to have comparable binding energies of 62.7 and 69.9 $kJ \cdot mol^{-1}$, respectively. The first binding site has a metal−oxygen distance of 2.15 Å and a slightly increased phosphorus−oxygen bond length of 1.49 Å (compared to 1.47 Å for MPA under vacuum), indicating that the bond has been weakened by the interaction with the zinc center. The second binding site has a much longer analogous interaction distance of 2.40 Å, with a secondary close contact of 2.63 Å between the second metal center and the hydroxyl oxygen. The phosphorus−oxygen bond is also weakened by this binding and has a value of 1.50 Å. Based upon these calculations and the experimental data, it is reasonable to assume that the MPA in **1** binds in a bridging fashion as there is no steric hinderance in the open channels of the title MOF.

In conclusion, we have successfully synthesized the first metal−organic replica of α-$PbO_2$ with coordinatedly unsaturated sites on its one-dimensional channel walls. More importantly, the title porous MOF exhibits an extremely high capacity for capture of the nerve agent surrogate methylphosphonic acid. These results may provide the basis for the development of next-generation MOF materials that can trap a wide range of chemical threat agents.

**Acknowledgment.** This work was financially supported by the National Basic Research Program of China (No. 2009CB939902) and LANL Director's funded postdoctoral LDRD Project # 20080780PRD2. We also would like to express our sincere thanks to the reviewers for their comments and constructive suggestions.

**Supporting Information Available:** Complete ref 2c, experimental procedures, analytical data, TGA, $N_2$ adsorption curve, and crystallographic data (cif, PDF). This material is available free of charge via the Internet at http://pubs.acs.org.

## References

(1) (a) Li, H.; Eddaoudi, M.; O'Keeffe, M.; Yaghi, O. M. *Nature* **1999**, *402*, 276–279. (b) Férey, G.; Mellot-Draznieks, C.; Serre, C.; Millange, F.; Dutour, J.; Surblé, S.; Margiolaki, I. *Science* **2005**, *305*, 2040–2042. (c) Kitagawa, S.; Kitaura, R.; Noro, S. *Angew. Chem., Int. Ed.* **2004**, *43*, 2334–2375. (d) Lee, J. Y.; Farha, O. K.; Roberts, J.; Scheidt, K. A.; Nguyen, S. T.; Hupp, J. T. *Chem. Soc. Rev.* **2009**, *38*, 1450–1459. (e) Perry, J. J.; Perman, J. A.; Zaworotko, M. J. *Chem. Soc. Rev.* **2009**, *38*, 1400–1417. (f) Long, J. R.; Yaghi, O. M. *Chem. Soc. Rev.* **2009**, *38*, 1213–1214. (g) Czaja, A. U.; Trukhan, N.; Müller, U. *Chem. Soc. Rev.* **2009**, *38*, 1284–1293.

(2) (a) Li, J. R.; Kuppler, R. J.; Zhou, H.-C. *Chem. Soc. Rev.* **2009**, *38*, 1477–1504. (b) Li, K. H.; Olson, D. H.; Seidel, J.; Emge, T. J.; Gong, H. W.; Zeng, H. P.; Li, J. *J. Am. Chem. Soc.* **2009**, *131*, 10368–10369. (c) Park, Y. K.; et al. *Angew. Chem., Int. Ed.* **2007**, *46*, 8230–8233. (d) Huang, X. C.; Lin, Y. Y.; Zhang, J. P.; Chen, X. M. *Angew. Chem., Int. Ed.* **2006**, *45*, 1557–1559. (e) Allendorf, M. D.; Bauer, C. A.; Bhakta, R. K.; Houk, R. J. T. *Chem. Soc. Rev.* **2009**, *38*, 1330–1352. (f) Shimizu, G. K. H.; Vaidhyanathan, R.; Taylor, J. M. *Chem. Soc. Rev.* **2009**, *38*, 1430–1449. (g) Ma, L.; Abney, C.; Lin, W. *Chem. Soc. Rev.* **2009**, *38*, 1248–1256. (h) Düren, T.; Bae, Y. S.; Snurr, R. Q. *Chem. Soc. Rev.* **2009**, *38*, 1237–1247.

(3) Férey, G.; Mellot-Draznieks, C.; Serre, C.; Millange, F. *Acc. Chem. Res.* **2005**, *38*, 217–225.

(4) Rowsell, J. L. C.; Spencer, E. C.; Eckert, J.; Howard, J. A. K.; Yaghi, O. M. *Science* **2005**, *309*, 1350–1354.

(5) Banerjee, R.; Phan, A.; Wang, B.; Knobler, C.; Furukawa, H.; O'Keeffe, M.; Yaghi, O. M. *Science* **2008**, *319*, 939–943.

(6) (a) Britt, D.; Tranchemontagne, D.; Yaghi, O. M. *Proc. Natl. Acad. Sci. U.S.A.* **2004**, *101*, 7907–7912. (b) Cychosz, K. A.; Wong-Fog, A. G.; Matzger, A. J. *J. Am. Chem. Soc.* **2008**, *130*, 6938–6939. (c) Lan, A. J.; Li, K. H.; Wu, H. H.; Olson, D. H.; Emge, T. J.; Ki, W.; Hong, M.; Li, J. *Angew. Chem., Int. Ed.* **2009**, *48*, 2334–2338. (d) Zou, R. Q.; Sakarai, H.; Xu, Q. *Angew. Chem., Int. Ed.* **2006**, *45*, 2542–2546. (e) Zou, R. Q.; Sakurai, H.; Han, S.; Zhong, R. Q.; Xu, Q. *J. Am. Chem. Soc.* **2007**, *129*, 8402–8403.

(7) Hartshorn, C. M.; Singh, C. M.; Chang, E. L. *J. Mater. Chem.* **2002**, *12*, 602–605.

(8) Crystal data for **1**: space group $C222_1$, $a = 13.167(15)$ Å, $b = 17.558(19)$ Å, $c = 13.564(16)$ Å, $V = 3136(6)$ Å$^3$, $Z = 4$.

(9) See Supporting Information.

(10) O'Keefe, M.; Brese, N. E. *J. Am. Chem. Soc.* **1991**, *113*, 3226–3229.

(11) Implemented as the *PLATON* procedure: Spek, A. L. *A Multipurpose Crystallographic Tool*; Utrecht University: Utrecht, The Netherlands, 1998.

(12) (a) O'Keeffe, M.; Peskov, M. A.; Ramsden, S. J.; Yaghi, O. M. *Acc. Chem. Res.* **2008**, *41*, 1782–1789. (b) Delgado-Friedrichs, O.; O'Keeffe, M. *J. Solid State Chem.* **2005**, *178*, 2499–2504. (c) http://rcsr.anu.edu.au/rcsr_nets. (d) Wells, A. F. *Three-Dimensional Nets and Polyhedron*; Wiley: New

York, 1977. (e) Du, M.; Zhang, Z. H.; Tang, L. F.; Wang, X. G.; Zhao, X. J.; Batten, S. R. *Chem.—Eur. J.* **2007**, *13*, 2578–2586.
(13) Nelson, A. P.; Farha, O. K.; Mulfort, K. L.; Hupp, J. T. *J. Am. Chem. Soc.* **2009**, *131*, 458–460.
(14) Walton, K. S.; Snurr, R. Q. *J. Am. Chem. Soc.* **2007**, *129*, 8552–8556.
(15) Barja, B. C.; Jejedor-Jejedor, M. I.; Anderson, M. A. *Langmuir* **1999**, *15*, 2316–2321.
(16) The *ab* initio molecular simulation code CP2K can be found at http://cp2k.berlios.de/.
(17) (a) Goedecker, S.; Teter, M.; Hutter, J. *Phys. Rev. B* **1996**, *54*, 1703–1710. (b) Hartwigsen, C.; Goedecker, S.; Hutter, J. *Phys. Rev. B* **1998**, *58*, 3641–3662.

JA101440Z